Versatile triphenylphosphine-containing polymeric catalysts and elucidation of structure-function relationships

Matthew A. Sanders, Supraja S. Chittari, Nicole Sherman, Jack R. Foley, Abigail S. Knight*

Department of Chemistry, The University of North Carolina at Chapel Hill, Chapel Hill, North Carolina 27599, United States

Email: aknight@unc.edu

Abstract: Synthetic polymers are a modular solution to bridging the two most common classes of catalysts: proteins and small molecules. Polymers offer the synthetic versatility of small molecule catalysts, while simultaneously having the ability to construct microenvironments mimicking those of natural proteins. We synthesized a panel of polymeric catalysts containing a novel triphenylphosphine acrylamide monomer (TPPAm) and investigated how their properties impact the rate of a model Suzuki-Miyaura cross-coupling reaction. Systematic variation of polymer properties, such as molecular weight, functional density, and comonomer identity, led to tunable reaction rates and solvent compatibility, including full conversion in an aqueous medium. Studies with bulky substrates revealed connections between polymer parameters and reaction conditions that were further elucidated with a regression analysis. Some connections were substrate-specific, highlighting the value of the rapidly tunable polymer catalyst. Collectively, these results aid in building structure-function relationships to guide the development of polymer catalysts with tunable substrate and environment compatibility.

Introduction

Metalloenzymes exhibit remarkable selectivity and high turnover numbers in complex aqueous environments by aligning substrates in binding pockets with proximity to a reactive metal. Non-ligand residues in metalloenzymes provide structure that positions ligands and protects the metal center from off target reactivity.[1,2] However, ubiquitous and pharmaceutically relevant transformations such as C-C cross-coupling reactions are not catalyzed by natural enzymes. To fill this void, synthetic macromolecules including micellar,[3] cyclodextrin-derived,[4] and metal organic framework catalysts[5,6] have been developed, but challenges remain in achieving high reactivity at target conditions with noncovalent encapsulation strategies and heterogenous catalysts can be difficult to optimize. Proteins often function in mild conditions including low catalyst concentrations, exposure to ambient atmosphere, and aqueous solvent conditions; however, synthetic macromolecular catalysts frequently lack the structural complexity to protect a reactive metal and have limited aqueous solubility.[7–11]

Interest in developing macromolecular catalysts with desirable solvent compatibility and the ability to shield a reactive metal has motivated the development of polymeric catalysts for a variety of unnatural chemical reactions[12–15], such as copper(I)-catalyzed azide-alkyne cycloaddition,[16] selective oxidation,[17] palladium(II)-based pro-drug activation,[18] and DMF conversion to dimethylamines in the presence of sodium cyanide.[19] These studies further highlight the capabilities of synthetic macromolecular catalysts, and suggest that polymer properties such as monomer-substrate interactions, and secondary structure have a crucial impact on catalysis.[16–19]

However, an expanded set of design rules elucidating the significance of polymer properties, reaction conditions, and substrate, is needed to develop versatile catalysts that are compatible with application-specific reaction conditions.

Using the Suzuki-Miyaura cross-coupling as a model reaction, we describe systematic studies of polymeric catalysts to connect complex polymer composition to catalytic efficiency (Figure 1a). To address the growing interest in catalysts that are air and water-compatible,[20,21] we synthesized phosphine containing amphiphilic copolymers capable of ambient aqueous catalysis. Further, we probe how polymer composition parameters including molecular weight and comonomers impact both the catalytic yield and reaction rate. Finally, applying the modularity of polymeric catalysts, we have built a platform for rapid optimization and regression analysis to identify key chemical and physical parameters of the reaction. This will provide insight for further optimization and a general platform for future macromolecular catalyst development.

Results and Discussion

Triphenylphosphine acrylamide monomer (TPPAm) synthesis and copolymerization

Triphenylphosphine derived ligands are common in transition metal mediated catalysis,[22] and have been incorporated predominantly into styrene derived polymers through modification of

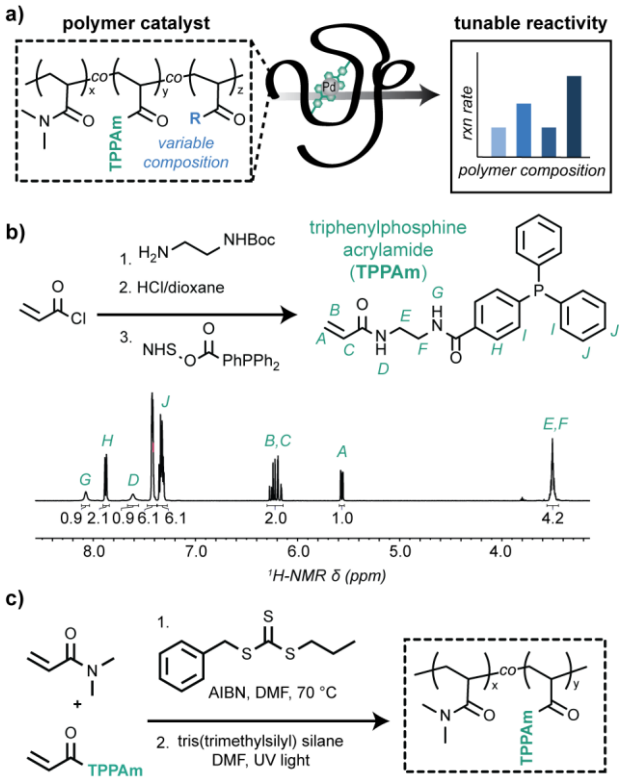

Figure 1. Triphenylphosphine acrylamide monomer (TPPAm) synthesis and copolymerization. a) Schematic illustrating that macromolecule catalyst structure impacts reaction rate. b) Schematic of the TPPAm monomer synthesis and resulting ^{1}H-NMR spectrum of the purified product. c) Polymerization schematic for DMA-TPPAm copolymers

Merrifield resins.[23] To develop polymers with a breadth of compositions, we synthesized a triphenylphosphine acrylamide monomer (TPPAm), that is compatible with controlled radical polymerization methods and a wide monomer scope (Figure 1a). The synthesis was accomplished via substitution of acryloyl chloride with a mono Boc-protected ethylenediamine followed by a Boc deprotection and amide coupling to the NHS ester of 4-(diphenylphosphino)benzoic acid (Figures 1b, S21-28).

Preliminary characterization of the catalytic efficacy was performed with statistical copolymers of TPPAm and dimethylacrylamide (DMA), a monomer with limited potential interactions with palladium (Figure 1c). Reversible addition-fragmentation chain transfer (RAFT) polymerization in DMF yielded polymers of controlled molecular weight (M_n), low dispersity (Đ), and similar rates of monomer incorporation leading to approximately statistical copolymers (Figure S1-6).[24] Polymeric catalyst, P1, was synthesized with 5 mol% TPPAm to facilitate catalysis while having a limited impact on solution polymer structure (Table 1). As trithiocarbonates can form complexes with palladium,[25,26] we removed the trithiocarbonate end group using tris(trimethylsilyl)silane as a proton capping agent.[27] Upon confirmation of trithiocarbonate removal by ^{1}H-NMR (Figure S7), we complexed P1 to palladium using dichloro(1,5-cyclooctadiene)palladium as the metal source in dilute solution.[28] Following precipitation, complete consumption of unbound triphenylphosphine was confirmed by observing a peak shift in a ^{31}P-NMR spectrum from a single peak at -6 ppm to peaks between 25-35 ppm. This shift

Polymer label	Mol% additive monomers	Monomer feed ratio (mol%)	Target molecular weight (kDa)	Monomer ratio (^{1}H-NMR, mol%)	Molecular weight (^{1}H-NMR, kDa)	Đ (SEC)
P1	5% TPPAm	95:5	25,000	95:5	23,000	1.16
P8kDa	5% TPPAm	95:5	7,500	96:4	8,100	1.16
P13kDa	5% TPPAm	95:5	13,500	96:4	13,000	1.11
P37kDa	5% TPPAm	95:5	37,500	96:4	37,000	1.20
P47kDa	5% TPPAm	95:5	50,000	96:4	47,000	1.27
P76kDa	5% TPPAm	95:5	75,000	95:5	76,000	1.47
P2.5%	2.5% TPPAm	97.5:2.5	25,000	97:3	26,000	1.13
P7.5%	7.5% TPPAm	92.5:7.5	25,000	92:8	26,000	1.17
P10%	10% TPPAm	90:10	25,000	90:10	26,000	1.17
PNAM	5% TPPAm, 47.5% NAM	47.5:47.5:5	25,000	48:47:5	26,000	1.16
PHEAA	5% TPPAm, 47.5% HEAA	47.5:47.5:5	25,000	47:48:5	25,000	1.25
PPEGA	5% TPPAm, 47.5% PEGA	47.5:47.5:5	25,000	48:47:5	25,000	1.14
PBAA	5% TPPAm, 15% BAA	80:15:5	25,000	80:15:5	25,000	1.18

Table 1. ^{1}H-NMR and DMF SEC characterization of polymer catalysts. Remaining monomer mol% is DMA for all polymers. Monomer abbreviations: *N*-acryloylmorpholine (NAM) hydroxyethyl acrylamide (HEAA), poly(ethylene glycol) methyl ether acrylate (PEGA), and benzyl acrylamide (BAA).

indicates triphenylphosphine moieties are bound to palladium indicating the synthesis of the catalyst complex P1 (Figure S8).[29]

As a model reaction, a Suzuki-Miyaura cross-coupling between 4-bromofluorobenzene and phenylboronic acid was selected to easily monitor reaction progression using ^{19}F-NMR (Figure 2a).[30] A common solvent mixture of 1:1 DMF:H_2O was implemented to enable comparisons

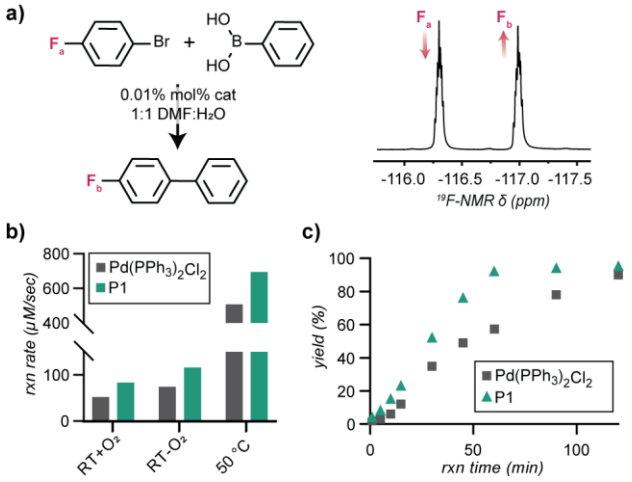

Figure 2. A model reaction for comparing macromolecular catalyst P1 to bis(triphenylphosphine)palladium dichloride ($Pd(PPh_3)_2Cl_2$). a) Suzuki cross-coupling reaction scheme and ^{19}F-NMR spectrum mid-reaction (30 min, ambient temperature and atmosphere, P1). b) Reaction rates of $Pd(PPh_3)_2Cl_2$ (grey) and P1 (green) at various reaction conditions. Standard error values from the calculated slope are too low to visualize on the plot. c) Plot of yield vs reaction time comparing $Pd(PPh_3)_2Cl_2$ (grey) and P1 (green) at room temperature and ambient conditions. All reactions were run with 0.3 M 4-bromofluorobenzene and all time points were separate reactions.

between macromolecular and small molecules catalysts. Catalyst P1 was compared to a small molecule mimic, bis(triphenylphosphine)palladium(II) dichloride ($Pd(PPh_3)_2Cl_2$). To calculate Pd loading for polymeric catalysts, we assumed 2:1 coordination of phosphine ligands (as calculated from NMR) to Pd. At equal palladium concentrations of 0.01 mol%, P1 outperforms $Pd(PPh_3)_2Cl_2$ under common conditions: inert atmosphere, ambient and elevated temperature (50 °C), and added potassium carbonate (3 equiv) (Figures 2b and S10-11).[22] To confirm that this reactivity is dependent on triphenylphosphine coordination to Pd, we synthesized a DMA homopolymer lacking TPPAm. After complexation, no reactivity was observed over two hours during which a reaction with catalyst P1 reaches >95% conversion (Figure S9).

Ambient reaction conditions and catalyst stability are relevant to both biocatalysis and industrial reaction optimization. We evaluated the catalytic efficacy at room temperature in both the presence and absence of oxygen and P1 outperformed the analogous small molecule, $Pd(PPh_3)_2Cl_2$ in both conditions (Figure 2c, S10). As palladium catalysts often need to be stored in air-free environments for long term stability, we tested the stability of catalyst P1 at ambient

conditions by measuring the reaction rate after 7 months of benchtop storage and observed limited difference in the reaction rate (84 vs 85 µM/sec) (Table S2). Further, P1 displayed stability in solution as well: after storing the catalyst in 1:1 DMF:H_2O at ambient conditions for 24 h, only a modest decrease in cross-coupling yield from >95% to 87% was observed after 2 h. From these results, we demonstrate that the polymeric catalyst both outperforms a small molecule analogue in reaction efficiency and demonstrates remarkable catalyst stability.

Impact of polymer properties on catalyst efficacy

Motivated by the impact of hierarchical structure on natural metalloenzyme efficiency, we sought to understand the impact of changing the polymer matrix (i.e., molecular weight and comonomer) on reaction rate. Tuning the molecular weight modulates the number of palladium sites per polymer without changing the density within a single polymer. We synthesized DMA:TPPAm (95:5) copolymers with molecular weights from 8 to 76 kDa (P8kDa-P76kDa, Table 1, Figure S4), targeting single chain assemblies that would remain soluble. Dynamic light scattering (DLS) confirmed minimal aggregation in this molecular weight range at concentrations above those used for catalysis (1 mg/mL, Figure S12). At a constant loading of Pd (0.01 mol%), we observed that as molecular weight increases from 8 to 47 kDa, the reaction rate increased from 64 to 141 µM/sec, a 2.2-fold increase (Figures 3a and S13, Table S2).[12,16] However, after increasing the molecular weight further to 76 kDa, the rate of reaction decreased

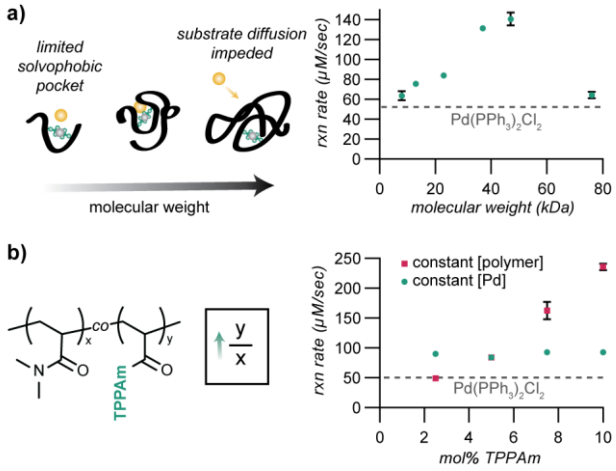

Figure 3. Varying the number of reactive sites within a polymer. (a) Schematic illustrating hypothesized impact of molecular weight on catalysis and a plot of reaction rate vs molecular weight for 95:5 DMA:TPPAm polymers at 0.01 mol%. (b) Schematic illustrating increased TPPAm:DMA ratio and a plot comparing mol% TPPAm to reaction rate for both a constant Pd loading (0.01 mol%, green) and constant polymer concentration [5.5 µM (equivalent to 0.01% loading of P1), red]. All reactions were run in 1:1 DMF:H_2O at 0.3M 4-bromofluorobenzene at room temperature and ambient conditions. In both plots the dashed line indicates the rate of reaction of bis(triphenylphosphine)palladium(II)dichloride ($Pd(PPh_3)_2Cl_2$). All error bars correspond to standard error of the calculated slope and all time points were separate reactions.

to 64 μM/sec. We hypothesized that lower molecular weights may not be able to fully form reactive pockets, whereas as the molecular weight increased above 47 kDa, substrate diffusion was prevented. Similar behavior with intermediate molecular weights yielding the highest reaction rates have been observed in the catalysis of azide-alkyne cycloadditions with a polymer catalyst.[16]

We hypothesized that increasing the TPPAm density could similarly increase the reaction rate of lower molecular weight polymers by generating a pocket through a higher density of Pd crosslinks. Polymers with molecular weights of 25 kDa with a 2.5-10 mol% of TPPAm (Table 1, P2.5%-P10% Figure S6) were compared at a constant Pd loading (0.01 mol%). Interestingly, these catalysts displayed very similar reactivity, with rates varying from 84 to 93 μM/sec (Figures 3b, S14, Table S2), indicating that cross-linking density had a minimal impact on reaction rate. However, when comparing the polymeric catalysts at a constant polymer concentration as opposed to a constant Pd concentration, the reaction rate increases from 49 μM/sec to 235 μM/sec. This is anticipated as the Pd loading increases from 0.005 mol% (P2.5%) to 0.02 mol% (P10%) (Table S3, Figure S15).

To expand the scope of intramolecular interactions available to the polymer scaffold, we selected four additional comonomers to include in the polymer catalysts. A hydrophilic monomer with a hydrogen bond donor (hydroxyethyl acrylamide, HEAA), two larger monomers [*N*-acryloylmorpholine**, (**NAM) and poly(ethylene glycol) methyl ether acrylate (M_n = 480, PEGA)], and a hydrophobic monomer (benzyl acrylamide, BAA) were selected. Each comonomer was

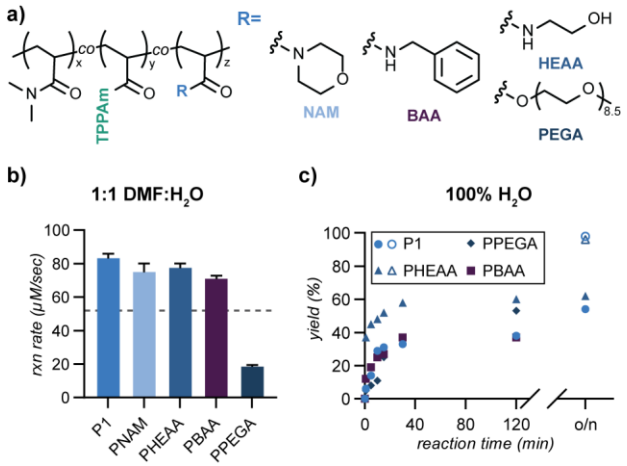

Figure 4. Expanding the monomer scope within the polymer catalysts. a) Schematic of copolymer structures. b) Plot of reaction rate versus comonomer identity in 1:1 DMF:H_2O with the dotted line indicating the rate of reaction of $Pd(PPh_3)_2Cl_2$. All reactions were 0.01 mol% Pd loading, 0.3 M 4-bromofluorobenzene, and ambient conditions. c) Aqueous catalysis reaction progression in 100% H_2O at 0.01 mol% Pd loading and 0.3 M 4-bromofluorobenzene (PNAM was insoluble in aqueous conditions). Unfilled circles correspond to 0.1 mol% Pd and 0.1 M 4-bromofluorobenzene concentration. All reactions were run at ambient conditions. All error bars correspond to standard error of the calculated slope and all time points were separate reactions.

incorporated at 47.5:47.5:5 feed ratio with comonomer:DMA:TPPAm, with the exception of BAA which was incorporated at 15:80:5 due to polymerization solubility limitations (Figure 4a, S6, Table 1).

These catalysts displayed similar reaction rates in 1:1 DMF:H_2O, aside from PPEGA. PPEGA reacted slower, likely due to the difficulty of substrate diffusion in the crowded environment (Figures 4b and S16, Table S2). Under biocompatible and environmentally inert aqueous conditions, the small molecule mimic ($Pd(PPh_3)_2Cl_2$) and PNAM were insoluble. However, the more hydrophilic copolymers PHEAA and PPEGA displayed modest yields of the desired biaryl (~60% yield, Figure 4c, S17), while P1 and PBAA copolymers performed with a lower yield (~40% yield Figure 4c, S17). The reactions in aqueous conditions were faster than those in the DMF:H_2O mixture, but never reached full conversion (Figure 4c). Increasing the catalyst concentration five- and ten-fold (0.05 and 0.1 mol% Pd) increased the overall yield (~70%) but did not result in full conversion (Figure S18); however, when the reaction with 0.1 mol% Pd was diluted, full conversion (>95%) was observed for the P1 and PHEAA catalysts in aqueous conditions (Figure 4c, S19). This suggested that there is a limit to the solubility of the substrate-polymer complex in water and lowering the reaction concentration aids in solubility. Additionally, when a small volume of DMF (5% by volume) was added to the reaction at 0.01 mol% Pd loading, the reaction rate decreased but full conversion was again observed (Figure S20). The tunability of this polymer platform provides multiple strategies for optimization including tuning the molecular weight and improving aqueous yields via comonomer selection.

Optimizing reaction conditions for bulkier substrates

We identified that a variety of polymer properties including molecular weight and polymer composition impact the reaction rate and yield across conditions, and we thus sought to harness the modularity of the polymer platform to optimize reactions with bulkier substrates. Sterically encumbered boronic acids, 1-pyreneboronic acid and 1-naphthylboronic acid, were selected to facilitate continued monitoring via ^{19}F-NMR. We chose to exploit the modularity of our polymeric system with Design of Experiments to optimize multiple variables simultaneously as opposed to traditional iterative screening.[31–34] Under consistent ambient atmosphere, initial variables included temperature, organic solvent, water concentration, reaction concentration, and polymer composition, as each has been demonstrated to impact the reaction efficacy.[22,35–37] These variables were incorporated into a factor screening experiment designed using JMP (Figure 5a, Table S4). Only one initial reaction condition (0.3 M 4-bromofluorobenzene, ethanol:H_2O 9:1, 50 °C, PBAA) generated observable product after 30 min for both substrates, reaching higher yields than $Pd(PPh_3)_2Cl_2$ at the same conditions (Table S5). To select conditions for a second round of optimization, ethanol was selected as the sole organic solvent and 12 additional conditions were generated with JMP to further span the reaction space (Table S6). For each of the reactions that had an observable yield at 30 min, the final yield after 72 h was measured. Following optimization, a yield of 64% (0.3M 4-bromofluorobenzene, ethanol:H_2O 9:1, 65 °C, P1) and 79% (0.3 M 4-bromofluorobenzene, ethanol:H2O 9:1, 65 °C, PHEAA) were obtained for the pyrenyl and napthyl substrates respectively.

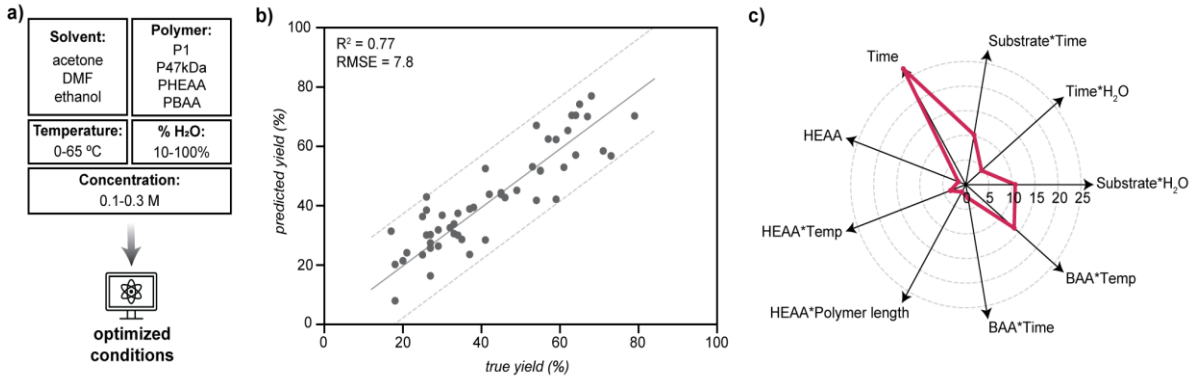

Figure 5. Optimization design and statistical modeling of reaction parameters. a) Parameters for optimization of reaction conditions. b) A linear regression algorithm with quadratic interaction terms modeling true vs predicted yields for 52 reactions. Dashed lines represent a 95% confident interval. c) Model coefficients with statistically significant ($p<0.05$, except HEAA, HEAA*length, and time*BAA with $p<0.1$) correlation to yield. Only magnitudes of values are plotted with larger magnitude indicating greater impact.

These yields were encouraging, and we wanted to further investigate how each variable impacted the reaction efficacy. Linear regression models have successfully predicted both regioselectivity and optimal reaction conditions for small molecule catalysts.[38,39] Therefore, we applied a linear regression algorithm with quadratic interaction terms to identify correlations between the measured yield and reaction variables, including descriptors of polymer composition and length. Model coefficients also describe the strength of the correlation between a variable and reaction yield. Larger magnitude coefficients describe stronger effects and the sign of the coefficient, positive or negative, describe a beneficial or diminishing contribution, respectively. The model was also iteratively cross-validated by inputting some known out-of-sample reaction conditions, predicting the reaction yield, and comparing to the measured yield (Figure 5b). This cross-validation showed a goodness-of-fit R^2 value of 0.77, indicating that the model was a predictive to moderate accuracy and thus likely contained meaningful coefficients for examination. We therefore calculated p-values and standard deviations for model coefficients and found several coefficients with $p<0.05$, including some with chemical relevance (Figure 5c, Table S7). The largest coefficient is reaction time that demonstrates a greater yield with longer times, as anticipated. The water*time coefficient describes diminishing benefit in increasing reaction time with higher water content. Other reaction conditions, such as substrate*water, reveal that with the pyrenyl substrate, increased water content is less preferred, while the naphthyl substrate is comparatively higher yielding with increased water concentration. We hypothesize that since the pyrenyl substrate is significantly more hydrophobic, the increased water content, while solubilizing the carbonate base, limits reactivity.[37] Another interesting interaction term, substrate*time, demonstrates less benefit for increased reaction time for pyrenyl versus the napthyl substrate. Interestingly, some descriptors of polymer composition, parameterized by mole fractions of their incorporation, appear in interaction terms with reaction conditions, such as HEAA*temperature and BAA*temperature. Increased temperature more positively impacts PBAA compared to PHEAA, and we hypothesize the increased diffusion rate at higher temperatures is more valuable for the more hydrophobic copolymer.

Other interaction terms with polymer composition, although significant only to $p<0.1$ (Figure 5c, Table S7), also show some promising trends with reaction rate. The positive coefficients for HEAA and HEAA*polymer length suggest a global increase in yield with the addition of a hydrophilic comonomer to the polymeric catalyst, with particular benefit for longer polymers. A negative coefficient for time*BAA may suggest that more hydrophobic polymeric catalysts show diminishing benefits from longer reaction times.

This screening approach rapidly identified reaction conditions for the optimization of Suzuki-Miyaura cross-coupling reactions. Through analysis of model coefficients, we deconvolute a complex dialogue between reaction parameters and yield, including unique factor interactions between water content and substrate type as well as contributions from polymeric catalyst structure. The regression model described here represents a first step towards a larger goal in optimizing a polymeric catalyst system with highly tunable reaction parameters. This contributes to the rapidly expanding dialogue between more advanced regression models in machine learning and both polymeric design[40] and catalyst design,[41] demonstrating the potential in bridging these fields.

Conclusion.

We have developed a platform of palladium cross-linked polymer catalysts to probe the structure-function relationships between polymer properties and catalyst performance for a model Suzuki-Miyaura cross-coupling reaction both in organic and aqueous conditions. Increasing reaction rate with higher molecular weight polymers was observed in addition to aqueous compatibility with comonomer addition. Finally, we described a model that optimizes reaction conditions and identifies relationships between chemical and physical reaction parameters.

Synthetic macromolecules offer potential as catalytic nanoreactors that mimic natural enzymes by imbuing internal structure.[42] Further incorporation of hierarchical structure through covalent or electrostatic cross-links, sequence definition,[43] as well as helical-[28] or β-sheet-like[44] moieties will continue to expand the toolbox for improving polymer catalyst efficacy. These advances will aid in the synthesis of macromolecules that rival complex small molecules and natural enzymes in both reactivity and selectivity.

ACKNOWLEDGMENT

This work is supported by the donors of the American Chemical Society Petroleum Research Fund under award 61293-DN17. SSC is supported by the National Science Foundation under award DGE-2040435. M.A.S thanks the UNC Burroughs-Wellcome fellowship for a semester funding award. We acknowledge support from the UNC Macromolecular Interactions Facility in DLS experiments. The facility is supported in part by the National Cancer Institute of the National Institutes of Health under award number P30CA016086. We acknowledge the UNC Department of Chemistry Mass Spectrometry Core Laboratory (HRMS is supported by the National Science Foundation under Grant No. CHE-1726291), and the NMR core laboratory staff Drs. Marc ter Horst, Nuwanthika Dilrukshi, and Luke Fulton, supported by a National Science Foundation award number CHE-1828183. We thank the Gagne and Johnson research groups at UNC for valuable conversations.

References

(1) Chen, A. Y.; Adamek, R. N.; Dick, B. L.; Credille, C. V.; Morrison, C. N.; Cohen, S. M. Targeting Metalloenzymes for Therapeutic Intervention. *Chem. Rev.* **2019**, *119* (2), 1323–1455. https://doi.org/10.1021/acs.chemrev.8b00201.

(2) Zhao, M.; Wang, H.-B.; Ji, L.-N.; Mao, Z.-W. Insights into Metalloenzyme Microenvironments: Biomimetic Metal Complexes with a Functional Second Coordination Sphere. *Chem. Soc. Rev.* **2013**, *42* (21), 8360. https://doi.org/10.1039/c3cs60162e.

(3) La Sorella, G.; Strukul, G.; Scarso, A. Recent Advances in Catalysis in Micellar Media. *Green Chem.* **2015**, *17* (2), 644–683. https://doi.org/10.1039/c4gc01368a.

(4) Bai, C. C.; Tian, B. R.; Zhao, T.; Huang, Q.; Wang, Z. Z. Cyclodextrin-Catalyzed Organic Synthesis: Reactions, Mechanisms, and Applications. *Molecules* **2017**, *22* (9). https://doi.org/10.3390/molecules22091475.

(5) Wei, Y. S.; Zhang, M.; Zou, R.; Xu, Q. Metal-Organic Framework-Based Catalysts with Single Metal Sites. *Chem. Rev.* **2020**, *120* (21), 12089–12174. https://doi.org/10.1021/acs.chemrev.9b00757.

(6) Diyali, N.; Rasaily, S.; Biswas, B. Metal–Organic Framework: An Emergent Catalyst in C–N Cross-Coupling Reactions. *Coord. Chem. Rev.* **2022**, *469*, 214667. https://doi.org/10.1016/j.ccr.2022.214667.

(7) Schwizer, F.; Okamoto, Y.; Heinisch, T.; Gu, Y.; Pellizzoni, M. M.; Lebrun, V.; Reuter, R.; Köhler, V.; Lewis, J. C.; Ward, T. R. Artificial Metalloenzymes: Reaction Scope and Optimization Strategies. *Chem. Rev.* **2018**, *118* (1), 142–231. https://doi.org/10.1021/acs.chemrev.7b00014.

(8) Ilie, A.; Reetz, M. T. Directed Evolution of Artificial Metalloenzymes. *Isr. J. Chem.* **2015**, *55* (1), 51–60. https://doi.org/10.1002/ijch.201400087.

(9) Davis, H. J.; Ward, T. R. Artificial Metalloenzymes: Challenges and Opportunities. *ACS Cent. Sci.* **2019**, *5* (7), 1120–1136. https://doi.org/10.1021/acscentsci.9b00397.

(10) Deuss, P. J.; Denheeten, R.; Laan, W.; Kamer, P. C. J. Bioinspired Catalyst Design and Artificial Metalloenzymes. *Chem. - Eur. J.* **2011**, *17* (17), 4680–4698. https://doi.org/10.1002/chem.201003646.

(11) Clarke, C. J.; Tu, W.-C.; Levers, O.; Bröhl, A.; Hallett, J. P. Green and Sustainable Solvents in Chemical Processes. *Chem. Rev.* **2018**, *118* (2), 747–800. https://doi.org/10.1021/acs.chemrev.7b00571.

(12) Rubio-Cervilla, J.; González, E.; Pomposo, J. A. Advances in Single-Chain Nanoparticles for Catalysis Applications. *Nanomaterials* **2017**, *7* (10). https://doi.org/10.3390/nano7100341.

(13) Rothfuss, H.; Knöfel, N. D.; Roesky, P. W.; Barner-Kowollik, C. Single-Chain Nanoparticles as Catalytic Nanoreactors. *J. Am. Chem. Soc.* **2018**, *140* (18), 5875–5881. https://doi.org/10.1021/jacs.8b02135.

(14) Chen, J.; Garcia, E. S.; Zimmerman, S. C. Intramolecularly Cross-Linked Polymers: From Structure to Function with Applications as Artificial Antibodies and Artificial Enzymes. *Acc. Chem. Res.* **2020**, *53* (6), 1244–1256. https://doi.org/10.1021/acs.accounts.0c00178.

(15) Barbee, M. H.; Wright, Z. M.; Allen, B. P.; Taylor, H. F.; Patteson, E. F.; Knight, A. S. Protein-Mimetic Self-Assembly with Synthetic Macromolecules. *Macromolecules* **2021**, *54* (8), 3585–3612. https://doi.org/10.1021/acs.macromol.0c02826.

(16) Chen, J.; Wang, J.; Bai, Y.; Li, K.; Garcia, E. S.; Ferguson, A. L.; Zimmerman, S. C. Enzyme-like Click Catalysis by a Copper-Containing Single-Chain Nanoparticle. *J. Am. Chem. Soc.* **2018**, *140* (42), 13695–13702. https://doi.org/10.1021/jacs.8b06875.
(17) Artar, M.; Souren, E. R. J.; Terashima, T.; Meijer, E. W.; Palmans, A. R. A. Single Chain Polymeric Nanoparticles as Selective Hydrophobic Reaction Spaces in Water. *ACS Macro Lett.* **2015**, *4* (10), 1099–1103. https://doi.org/10.1021/acsmacrolett.5b00652.
(18) Sathyan, A.; Croke, S.; Pérez-López, A. M.; de Waal, B. F. M.; Unciti-Broceta, A.; Palmans, A. R. A. Developing Pd(II) Based Amphiphilic Polymeric Nanoparticles for pro-Drug Activation in Complex Media. *Mol. Syst. Des. Eng.* **2022**, *7* (12), 1736–1748. https://doi.org/10.1039/D2ME00173J.
(19) Patenaude, B. F.; Berda, E. B.; Pazicni, S. Probing Secondary Coordination Sphere Interactions within Porphyrin-Cored Polymer Nanoparticles. *Polym. Chem.* **2022**, *13* (5), 677–683. https://doi.org/10.1039/D1PY01005K.
(20) Hooshmand, S. E.; Heidari, B.; Sedghi, R.; Varma, R. S. Recent Advances in the Suzuki–Miyaura Cross-Coupling Reaction Using Efficient Catalysts in Eco-Friendly Media. *Green Chem.* **2019**, *21* (3), 381–405. https://doi.org/10.1039/C8GC02860E.
(21) Polshettiwar, V.; Decottignies, A.; Len, C.; Fihri, A. Suzuki-Miyaura Cross-Coupling Reactions in Aqueous Media: Green and Sustainable Syntheses of Biaryls. *ChemSusChem* **2010**, *3* (5), 502–522. https://doi.org/10.1002/cssc.200900221.
(22) Miyaura, Norio.; Suzuki, Akira. Palladium-Catalyzed Cross-Coupling Reactions of Organoboron Compounds. *Chem. Rev.* **1995**, *95* (7), 2457–2483. https://doi.org/10.1021/cr00039a007.
(23) Guinó, M.; Hii, K. K. (Mimi). Applications of Phosphine-Functionalised Polymers in Organic Synthesis. *Chem Soc Rev* **2007**, *36* (4), 608–617. https://doi.org/10.1039/B603851B.
(24) Perrier, S. *50th Anniversary Perspective* : RAFT Polymerization—A User Guide. *Macromolecules* **2017**, *50* (19), 7433–7447. https://doi.org/10.1021/acs.macromol.7b00767.
(25) Fackler, J. P.; Seidel, W. C. Sulfur Ligand Complexes. IX. Reactions of Metal Xanthates and Their Derivatives. The Formation of Bisphosphine-Dithiocarbonate and -Trithiocarbonate Complexes of Palladium(II) and Platinum(II). *Inorg. Chem.* **1969**, *8* (8), 1631–1639. https://doi.org/10.1021/ic50078a012.
(26) Jones, P. G.; Sheldrick, G. M.; Usón, R.; Forniés, J.; Usón, M. A. Dithiocarbonate and Trithiocarbonate Complexes of Palladium(II); Crystal Structure of Pd(Ph3P)2(CS20) CH2C12. 5.
(27) Moad, G.; Rizzardo, E.; Thang, S. H. End-Functional Polymers, Thiocarbonylthio Group Removal/Transformation and Reversible Addition-Fragmentation-Chain Transfer (RAFT) Polymerization: Thiocarbonylthio Group Removal/Transformation. *Polym. Int.* **2011**, *60* (1), 9–25. https://doi.org/10.1002/pi.2988.
(28) Willenbacher, J.; Altintas, O.; Roesky, P. W.; Barner-Kowollik, C. Single-Chain Self-Folding of Synthetic Polymers Induced by Metal-Ligand Complexation. *Macromol. Rapid Commun.* **2013**, *35* (1), 45–51. https://doi.org/10.1002/marc.
(29) Pons, J.; García-Antón, J.; Solans, X.; Font-Bardia, M.; Ros, J. *Trans* -Dichloridobis(Triphenylphosphine)Palladium(II)In Memory of Professor Xavier Solans i Huguet, Deceased September 3, 2007. *Acta Crystallogr. Sect. E Struct. Rep. Online* **2008**, *64* (5), m621–m621. https://doi.org/10.1107/S1600536808008337.

(30) Zientek, N.; Laurain, C.; Meyer, K.; Kraume, M.; Guthausen, G.; Maiwald, M. Simultaneous 19F–1H Medium Resolution NMR Spectroscopy for Online Reaction Monitoring. *J. Magn. Reson.* **2014**, *249*, 53–62. https://doi.org/10.1016/j.jmr.2014.10.007.
(31) Weissman, S. A.; Anderson, N. G. Design of Experiments (DoE) and Process Optimization. A Review of Recent Publications. *Org. Process Res. Dev.* **2015**, *19* (11), 1605–1633. https://doi.org/10.1021/op500169m.
(32) Kucmierczyk, P.; Duehren, R.; Sang, R.; Jackstell, R.; Beller, M.; Franke, R. Palladium-Catalyzed Methoxycarbonylation Investigated by Design of Experiments. **2022**, 9.
(33) Denmark, S. E.; Butler, C. R. Vinylation of Aromatic Halides Using Inexpensive Organosilicon Reagents. Illustration of Design of Experiment Protocols. *J. Am. Chem. Soc.* **2008**, *130* (11), 3690–3704. https://doi.org/10.1021/ja7100888.
(34) Bobers, J.; Hahn, L. K.; Averbeck, T.; Brunschweiger, A.; Kockmann, N. Reaction Optimization of a Suzuki-Miyaura Cross-Coupling Using Design of Experiments. *Chem. Ing. Tech.* **2022**, *94* (5), 780–785. https://doi.org/10.1002/cite.202100194.
(35) Kotha, S.; Lahiri, K.; Kashinath, D. Recent Applications of the Suzuki – Miyaura Cross-Coupling Reaction in Organic Synthesis. **2002**, 63.
(36) Bellina, Pf.; Carpita, A.; Rossi, R. Palladium Catalysts for the Suzuki Cross-Coupling Reaction: An Overview of Recent Advances. *N. Y.* **2004**, No. 15.
(37) Mondal, M.; Bora, U. An Efficient Protocol for Palladium-Catalyzed Ligand-Free Suzuki–Miyaura Coupling in Water. *Green Chem.* **2012**, *14* (7), 1873. https://doi.org/10.1039/c2gc35401b.
(38) Werth, J.; Sigman, M. S. Linear Regression Model Development for Analysis of Asymmetric Copper-Bisoxazoline Catalysis. *ACS Catal.* **2021**, *11* (7), 3916–3922. https://doi.org/10.1021/acscatal.1c00531.
(39) Sigman, M. S.; Harper, K. C.; Bess, E. N.; Milo, A. The Development of Multidimensional Analysis Tools for Asymmetric Catalysis and Beyond. *Acc. Chem. Res.* **2016**, *49* (6), 1292–1301. https://doi.org/10.1021/acs.accounts.6b00194.
(40) Gormley, A. J.; Webb, M. A. Machine Learning in Combinatorial Polymer Chemistry. *Nat. Rev. Mater.* **2021**, *6* (8), 642–644. https://doi.org/10.1038/s41578-021-00282-3.
(41) Yang, W.; Fidelis, T. T.; Sun, W.-H. Machine Learning in Catalysis, From Proposal to Practicing. *ACS Omega* **2020**, *5* (1), 83–88. https://doi.org/10.1021/acsomega.9b03673.
(42) González-Burgos, M.; Asenjo-Sanz, I.; Pomposo, J. A.; Radulescu, A.; Ivanova, O.; Pasini, S.; Arbe, A.; Colmenero, J. Structure and Dynamics of Irreversible Single-Chain Nanoparticles in Dilute Solution. A Neutron Scattering Investigation. *Macromolecules* **2020**, *53* (18), 8068–8082. https://doi.org/10.1021/acs.macromol.0c01451.
(43) De Neve, J.; Haven, J. J.; Maes, L.; Junkers, T. Sequence-Definition from Controlled Polymerization: The next Generation of Materials. *Polym. Chem.* **2018**, *9* (38), 4692–4705. https://doi.org/10.1039/C8PY01190G.
(44) Warren, J. L.; Dykeman-Bermingham, P. A.; Knight, A. S. Controlling Amphiphilic Polymer Folding beyond the Primary Structure with Protein-Mimetic Di(Phenylalanine). *J. Am. Chem. Soc.* **2021**, jacs.1c05659. https://doi.org/10.1021/jacs.1c05659.